ELSEVIER

Tectonophysics 247 (1995) 239–254

TECTONOPHYSICS

Frictional rheology: hardening by rotation of active normal faults

Amotz Agnon *, Ze'ev Reches

Institute of Earth Sciences, The Hebrew University, Jerusalem 91904, Israel

Received 3 May 1994; revised version accepted 5 September 1994

Abstract

A simple model for work-hardening associated with rotation of active normal faults around horizontal axes mimics features of extended regions. We use Mohr–Coulomb envelopes to derive a frictional rheology for the upper crust. Sliding on block-bounding faults is assumed to constrain the stress state in the upper crust regardless of the deformation within the blocks. The model predicts that the stress-strain relations at a constant depth will be saw-toothed in shape with stages of gradual work-hardening following events of abrupt softening. The rupture of faults at the weakest zone in the loaded crust corresponds to the softening stage that is followed by work-hardening due to local block rotation. Work-hardening can drive lateral distribution of tectonic extension to form large extended regions with many domains of tilted blocks (Basin and Range type). In a thinning crust, however, material points undergo shallowing and the work-hardening is moderated by the effect of shallowing that decrease the frictional resistance. We use experimentally derived parameters of strength and friction to quantify the model predictions and to analyze the distribution of extension in Basin and Range and the frequency of tilt values in this region.

1. Introduction

High extensional strains are frequently manifested by rotation of crustal blocks. While blocks of the shallow sedimentary cover may rotate by glide on curved normal faults, several recent studies indicate that planar normal faults dominate at depth. Deep reflection imaging in extensional regions show mainly planar reflectors in the sedimentary sections (Jackson et al., 1988; Thompson et al., 1989; Smith et al., 1989; Roberts and Yielding, 1991; Yielding et al., 1991; Brun et al., 1991). Stein and Barrientos (1985) combine hypocenter distribution with geodetic data to lack of curvature in a Basin and Range earthquake. Studies of distributions of hypocenters with depth in other regions preferred planar active normal faults throughout the seismogenic layer (Jackson, 1987; Deverchere and Houdry, 1993). Deep normal fault events typically show dips in excess of 60° and always higher than 40° (Jackson, 1987; Thatcher and Hill, 1991; Doser and Yarwood, 1993). Although low-angle seismic reflections are observed, these are not necessarily features of active frictional sliding.

Rotation of blocks bounded by planar normal faults can be achieved by 'domino' or 'book shelf' style (Figs. 1,2) (Proffett, 1977; Garfunkel and Bartov, 1977; Stewart, 1980; Jackson et al., 1988;

* Corresponding author.

SSDI 0040-1951(94)00178-2

Le Pichon and Chamot-Rooke, 1991; Westaway, 1991). The activity of a rotating normal fault is limited by the angle between the fault plane and the principal stress axes. Once the angle of a fault plane decreases below a certain limit, the shear traction across the plane becomes insufficient for driving further slip (Sibson, 1985; Nur et al., 1986). Therefore, reactivation of rotated faults that are inclined to their frictionally optimal orientations implies increase of the strength, or work-hardening of the faulted crust. In this paper we investigate the rheology of the faulted crust and analyze its implication to the formation of extensional regions. As the state of stress in the faulted crust is bound by the friction of its faults, we refer to the long-term response of the faulted crust as *frictional rheology*. We choose this term as it encompass the Mohr–Coulomb frictional strength criterion for granular materials, as well as the 'internal friction' characteristic of shear fracture of rocks (Handin, 1966, 1969; Reches and Lockner, 1994). The deformation of the upper crust is largely localized by slip on faults. Assuming that deformation of the upper crust requires overcoming friction on these faults, we seek a frictional rheology for describing the response of the crust to tectonic stresses.

Agnon and Eidelman (1991) have alluded to crustal block rotation as a mechanism which can contribute to work-hardening that controls litho-

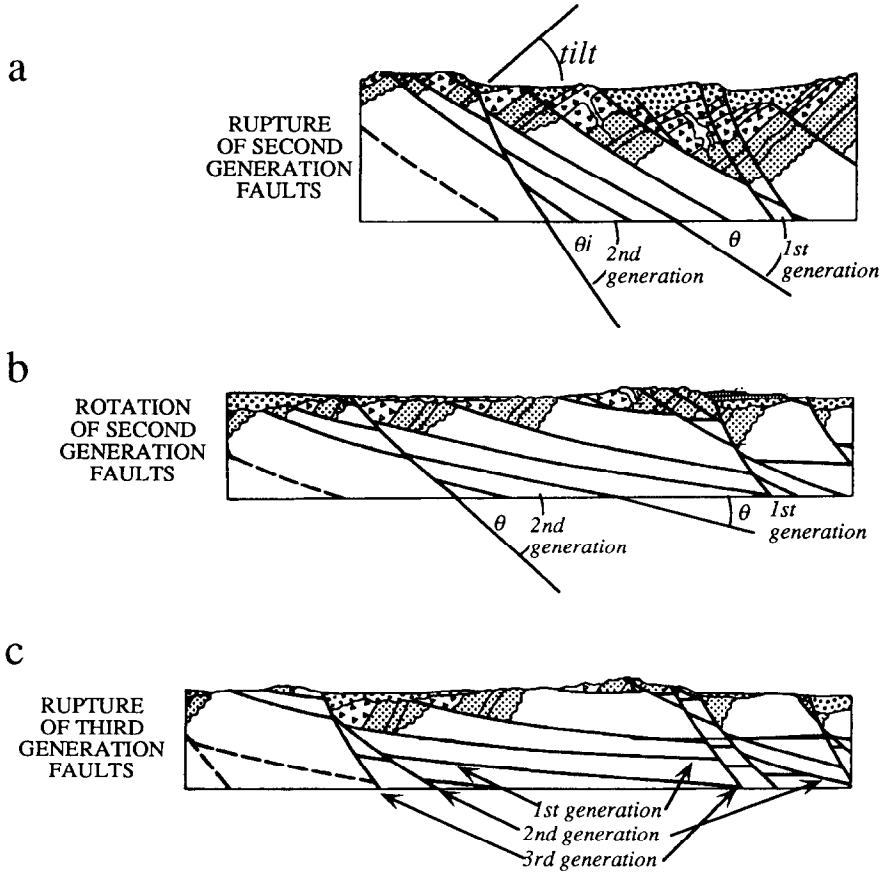

Fig. 1. Structural relations in the Yerington district, Basin and Range province, after Proffett (1977): (a) tilting of blocks, rotation and locking of normal faults, and second generation faulting; (b) slip on second generation faults and further rotation while locked first generation faults rotate passively; (c) third generation faulting.

spheric necking instabilities. As long as the material of the plate hardens sufficiently, the strength prohibits local necking under extension. So work-hardening may be responsible for the distribution of extensional deformation over wide regions such as the Basin and Range. This potential is interesting from a modeling point of view because distributed deformation is often attributed to the viscous rheology of the lithosphere (Sonder and England, 1986; Zuber et al., 1986; Buck, 1991).

Consider a thin plate loaded at the ends in extension at constant strain rate and decoupled from the substratum. The plate yields locally at the weakest available zone, and this local yielding unloads the rest of the plate. Sufficient work-hardening of the currently weakest domain drives the deformation away to the incumbent weakest domain. In this fashion the deformation migrates across a large region. Therefore, work-hardening may result in distributed finite deformation despite temporal localization in space. Work-hardening can drive migration of faulting and seismicity across extended regions on a variety of time scales. Intermittence of tectonic activity in materials that are governed by frictional rheology has no counterpart feature in viscoplastic materials, where diffusion controls the flow rates. Furthermore, unlike viscosity, friction depends only slightly on deformation rate and temperature (Byerlee, 1978). Unlike conventional metal plasticity, friction depends strongly on normal stress, or pressure. In addition frictional strength depends strongly on availability of slip planes, unlike continuum plasticity.

The frictional response of a faulted rock mass has been investigated in a variety of contexts. Reches (1979) showed that the gross strength of a faulted domain depends on the angular relations between the faults and the applied stresses and that softening and hardening stages are expected. Sibson (1985) derived an expression for the maximum rotation of active faults by implicitly assuming a constant mean stress. Nur et al. (1986) emphasized the role of the actual difference in cohesive strength of intact and faulted rock. Garfunkel (1989) derived a general expression for maximum angles of block rotation without specific assumptions on the parameters of the friction and brittle envelopes. These studies analyzed

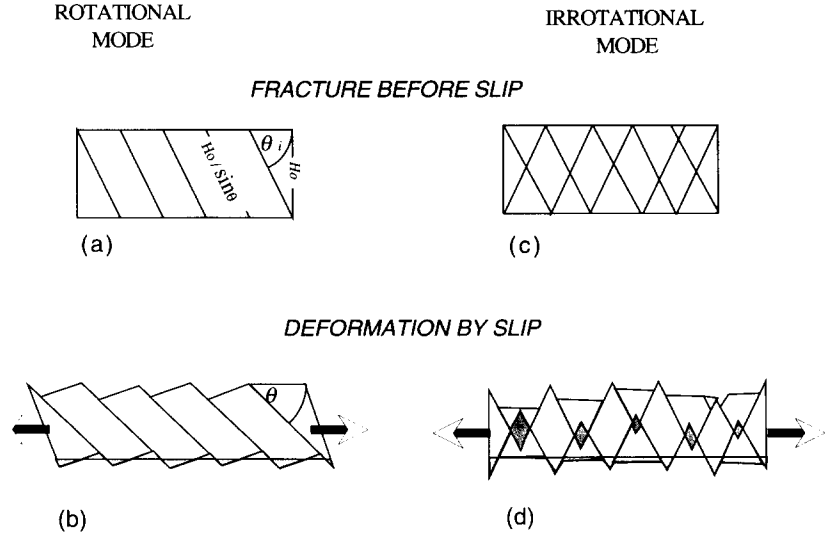

Fig. 2. Modes of large-scale deformation by slip along faults. *Rotational mode*: (a) a single set of faults; (b) block rotation by large displacements on a single set of faults, little distributed deformation at the block boundaries (shaded). *Non-rotational mode*: (c) a conjugate set of faults; (d) large displacements along the two sets of faults. The overlapping areas (shaded) show regions of expected higher internal deformation.

the response of a crust with preexisting faults organized in domains to further deformation. In the present study we address a general problem of tectonic evolution from faulting of an intact crust to the organization of fault domains, and finally to the long-term distribution of extension in the crust.

Much of the recent discussion on block rotation is focused on the validity of the rigid-block concept (Anders et al., 1993; Reches, 1994). Since we are concerned with the strength envelope, the internal deformation of the blocks is immaterial as long as the faults slip. Fault slip documents stresses reaching the slip criterion. We first reformulate the rotated fault problem for normal faults. We derive the long-term stress-strain relations typical of frictional response, and apply these relations to the two modes of large extensions: fault migration and second generation fault sets. Finally, we apply these modes to the observed patterns of extensional faults.

2. The model

The deformation in faulted areas is largely accommodated by sliding in coherently rotating domains (Freund, 1974; Garfunkel, 1974; Ron et al., 1984; Jackson et al., 1988). The active faults within each domain form a parallel set (Fig. 2a,b). We shall derive a frictional rheology that will mimic a simplified model for extension of the upper crust from a state of an intact brittle layer to an organized state of rotational domains. The mechanical response of the crust includes onset of faults, sliding along these faults, and the ensuing rotation of fault planes. We do not treat here the contribution of the lower ductile plate, and assume for simplicity that it adds a constant term to the strength of the plate. We explore the response of a brittle-ductile composite elsewhere (Agnon and Reches, 1991; Reches and Agnon, 1992).

2.1. Fundamental constitutive laws

The strength of the upper crust is bound by the strength of frictional sliding on faults (Goetze and Evans, 1979; Brace and Kohlstedt, 1980; McGarr, 1980; Dahlen, 1984). According to the adopted Mohr–Coulomb constitutive relation, sliding on a given surface is limited by the shear stress τ across that surface:

$$\tau \leqslant C_i + \mu_i \sigma_n \tag{1a}$$

$$\tau \leqslant C_f + \mu_f \sigma_n \tag{1b}$$

where C is the cohesion, μ is the coefficient of friction, and σ_n is the effective normal stress across the surface. The subscripts i and f refer to intact and faulted surfaces, respectively. Equation (1) implies that when the shear stress is lower than the strength (right-hand side) the fault does not slide. Conversely, when the fault slide, the shear stress equals the strength. In this quasi-static picture, the shear stress can not exceed the strength. Hence, one can infer the peak shear stresses from the activity of sliding. The blocks bounded by faults likely deform internally by small-scale faulting and folding (Anders et al., 1993; Reches, 1994), and this deformation may affect the loci and the timing of sliding on bounding faults. But the details of deformation within the blocks do not affect the upper bound of the stress imposed by the bounding faults. It follows that the stress evolution of a fault can be derived as long as its dip and depth during deformation are known.

The widely used strength envelopes of the crust are based on the assumption that faults are available at all orientations (Goetze and Evans, 1979; Brace and Kohlstedt, 1980). Therefore, faults at optimal orientations exist for any state of stress. Similarly, in a pile of loose sand slip surfaces can form in any orientation without breaking intact grains (e.g., Handin, 1969; Dahlen, 1984). Once a slip plane rotates away from its optimal orientation, a more favorably oriented plane may be activated and loose sand can flow under a constant state of stress. The situation is different in the upper crust where large-scale deformation is apparently accommodated by slip along few discrete fault surfaces of restricted orientations (Jackson et al., 1988; Thatcher and Hill, 1991). This localized mode dominates probably because random discontinuities in intact rocks

form rough surfaces dominated by asperities and cross-cutting intersections (Scholz, 1990). Rupture of asperities and intersections conceivably require higher stresses than the frictional strength of the few active faults.

2.2. Insight from geological observation

Freund (1974) recognized two modes of large-scale deformation by faulting in two dimensions: *rotational* mode, in which slip and rotation along a single set of active faults dominate the deformation (Fig. 2a,b), and *non-rotational* mode, in which two sets of active faults cross and displace each other (Fig. 2c,d). Strain increase by the non-rotational mode requires either continuous generation of new fault surfaces, or substantial plastic deformation within the blocks (Fig. 2c,d) (Oertel, 1965). Either of these processes demand widespread and pervasive rupturing of the blocks. On the other hand, strain increase by the rotational mode requires substantial plastic deformation at the margins of the deformed region (shaded in Fig. 2a,b), and relatively small deformation within the blocks.

Of the two modes depicted in Fig. 2, the rotational mode is more commonly observed in regions of distributed extension or shear. Bedding planes, remnant magnetization vectors, and micro-structural features on block bounding faults record the rotations (Proffett, 1977; Stewart, 1980; Ron et al., 1984, 1990). Active fault planes may rotate 30° or more around horizontal or vertical axes before a second-generation set of faults forms (Fig. 1) (Proffett, 1977; Ron et al., 1990). Combined block rotation and internal non-rotational deformation was observed in clay-cake experiments (Reches, 1988), and inferred for the Basin and Range Province (Anders et al., 1993).

The actual deformation path will be combined from increments of deformation at the mode that momentarily requires lowest stresses. We interpret the abundance of the rotational mode as indicating that the work-hardening in this mode is generally lower than in the non-rotational mode. The excess hardening of the non-rotational mode presumably drives the organization of crustal blocks into domains of coherently rotating subparallel faults. Finally, repetitive slip on a set of unfavorably oriented planes indicates that slip on an existing discontinuity is still easier than rupture of the intact rock on a crustal scale (Handin, 1969; Nur et al., 1986). Rupture of intact crust would occur only when the hardening by block rotation increases the strength along an existing fault to that of intact rocks.

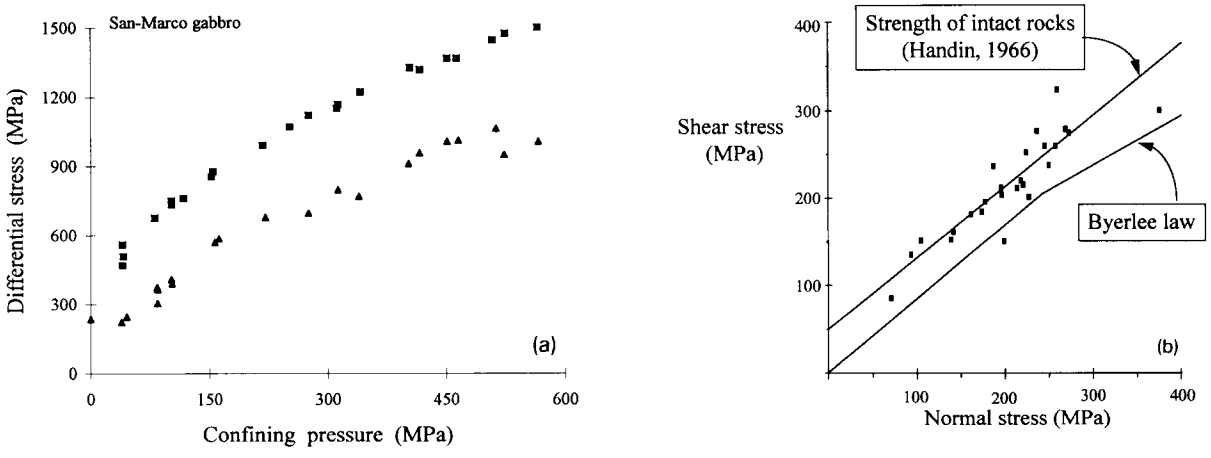

Fig. 3. (a) Strength of intact (squares) and saw-cut (triangles) gabbro as a function of confining pressure (after Stesky et al., 1974); (b) Failure and sliding strength of rocks (Mohr diagram space): square symbols denote failure for various rocks compiled from Handin (1966); straight line is a linear fit to the square symbols; lower segmented line is Byerlee law.

2.3. Experimental constraints

Consider an intact thin crustal plate loaded to rupture and then deforming by post-rupture slip along the newly formed set of faults. The key parameter in controlling the response is the strength difference between intact rocks and faulted rocks (Handin (1969). The detailed measurements of Stesky et al. (1974) on gabbro (Fig. 3a) indicated that the fracture strength of intact gabbro is higher than the frictional strength of faulted samples by over 300 MPa. Granites show an even higher strength difference of up to 600 MPa (Scholz, 1990, his fig. 1.12).

Figure 3b displays shear strength of 30 intact rock samples reported in Handin (1966) on a Mohr diagram. These samples include all faulting tests that yielded under brittle conditions: temperature of 150°C or below, pre-rupture strain smaller than 0.05, and measurable faulting angle. The samples include five specimens of basalt and gabbro, nine specimens of granite, gneiss and quartzite, five specimens of diorite and syenite, four specimens of peridotite and pyroxenite, and seven specimens of sedimentary rocks. This strength can be compared with the frictional resistance of rocks. Byerlee (1978) has demonstrated that, in general, the frictional resistance to slip in laboratory experiments does not depend on rock type, temperature, or strain rate. He showed that in many experiments:

$$\mu_f = 0.85 \quad C_f = 0 \text{ for } 3 < \sigma_n < 200 \text{ MPa} \qquad (2a)$$

$$\mu_f = 0.6 \quad C_f = 60 \text{ MPa for } \sigma_n > 200 \text{ MPa} \qquad (2b)$$

The frictional strength according to Byerlee Law is also shown in Fig. 3b as a segmented line. The least-squares fit of the strength of intact rock samples (Fig. 3b) suggests that the shear strength of intact rock is at least 50 MPa higher than rock faulted in the optimal orientation for slip.

2.4. Strength and work-hardening of faults

Consider a rectangular two-dimensional body that accommodates strain by slip and rotation of blocks along a single set of parallel faults (Fig. 2a). The two short boundaries of the deforming body may rotate, whereas the two long sides do not rotate (Reches, 1979; Garfunkel, 1989). The frictional strength of the faults (Eq. 1) determines the post-rupture yield stress of the model.

Rewriting the expression for τ and σ_n (1) in terms of the effective principal stresses, we obtain the differential stress required for slip on a fault whose normal is at an angle θ from σ_1 axis:

$$\Delta\sigma(\theta) = \sigma_1 - \sigma_3 = \frac{2(C_f + \mu_f\sigma_1)}{\sin 2\theta + \mu_f(1 - \cos 2\theta)} \qquad (3)$$

This expression is devised for extensional faulting in which σ_1, the maximum principal compressive stress, is vertical, and θ is the fault dip. The vertical stress is controlled by depth and the right-hand side of (3) depends explicitly on the vertical stress σ_1. In calculations the initial depth and the deformation path should be specified such that σ_1 is fully determined by the lithostatic overburden.

Strength of intact rock

We now examine the transition in the frictional medium from rupture of intact body to post-rupture slip and rotation. The orientation of the newly formed faults, θ_i, is controlled by a Mohr–Coulomb criterion (1a). This transition is illustrated in Fig. 4, using the same data as Fig.

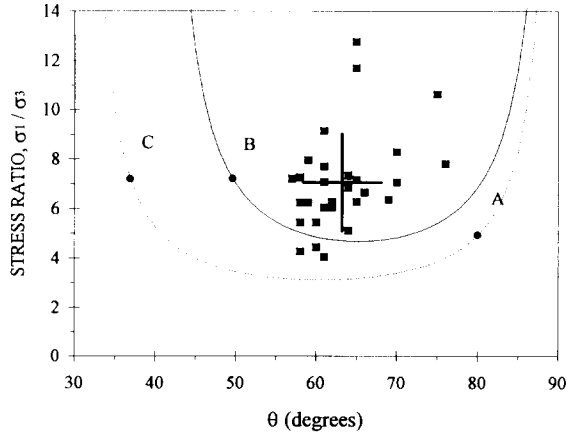

Fig. 4. Strength versus angle between the normal to rotating fault planes (θ in Fig. 2b) and the axis of maximum compressive stress. Solid squares denote failure for rocks of Fig. 3b; curves indicate strength according to Byerlee law; upper solid curve after (2a) and lower dotted curve after (2b).

3b (from Handin, 1966), in terms of the stress ratio σ_1/σ_3 versus fault angle θ. The mean value of σ_1/σ_3 with error bars shown as a cross in Fig. 4. The curves correspond to the stress ratio σ_1/σ_3 necessary to maintain slip along a fault inclined at the angle θ for Byerlee Law (2). For example, a ratio $\sigma_1/\sigma_3 \approx 5$ (point A in Fig. 4) is sufficient for slip along a fault whose normal is inclined at $\theta \approx 80°$ to σ_1 for high confining pressure (2b), but a ratio of about 7 is required to slip a fault with the same orientation for low confining pressure (solid curve in Fig. 4). The minimum of each curve is at angle $\theta_{min} = \arctan(\mu_f)/2 + 45°$.

Fig. 4 underscores two observations: First, the

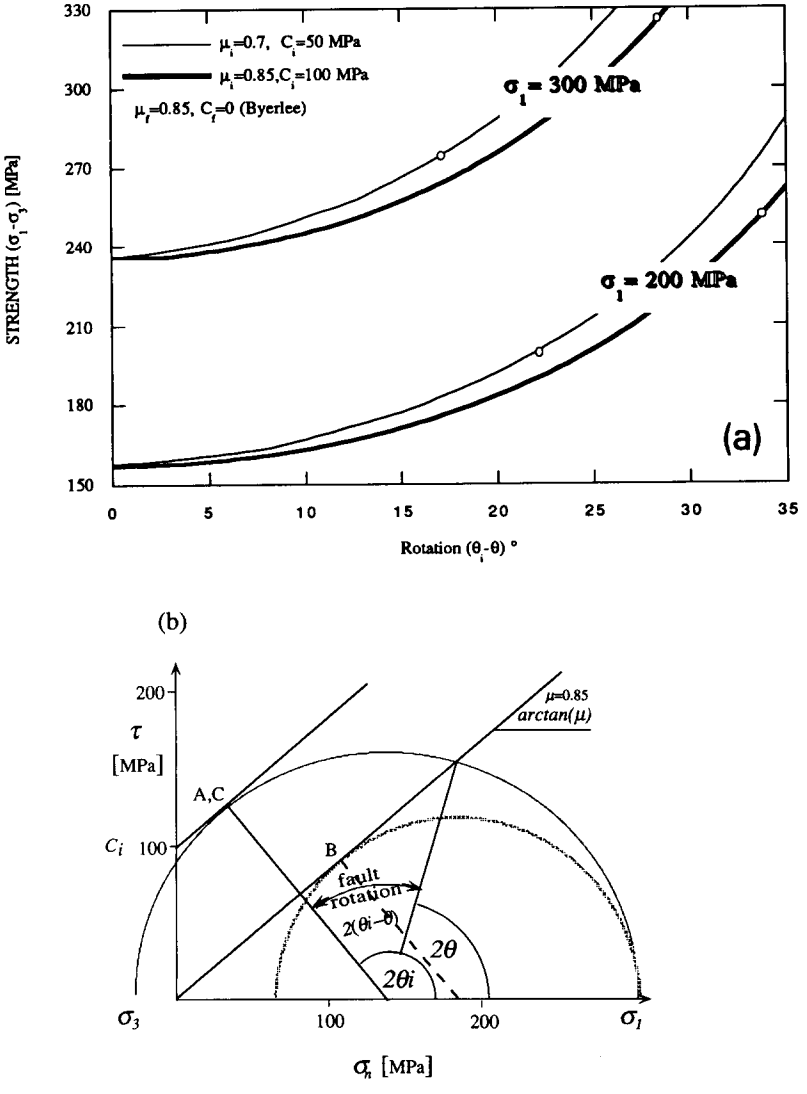

Fig. 5. The effect of rotation on the sliding strength of faults: (a) Strength versus rotation of normal faults for a range of parameters under invariant depth (see text for further details). (b) Mohr construction for pre- and post-rupture states of stress for normal faulting with constant σ_1. The least compressional stress σ_3 takes a negative value of -20 MPa prior to rupture, and it increases as extensional stress drops to 60 MPa (gray circle) after rupture.

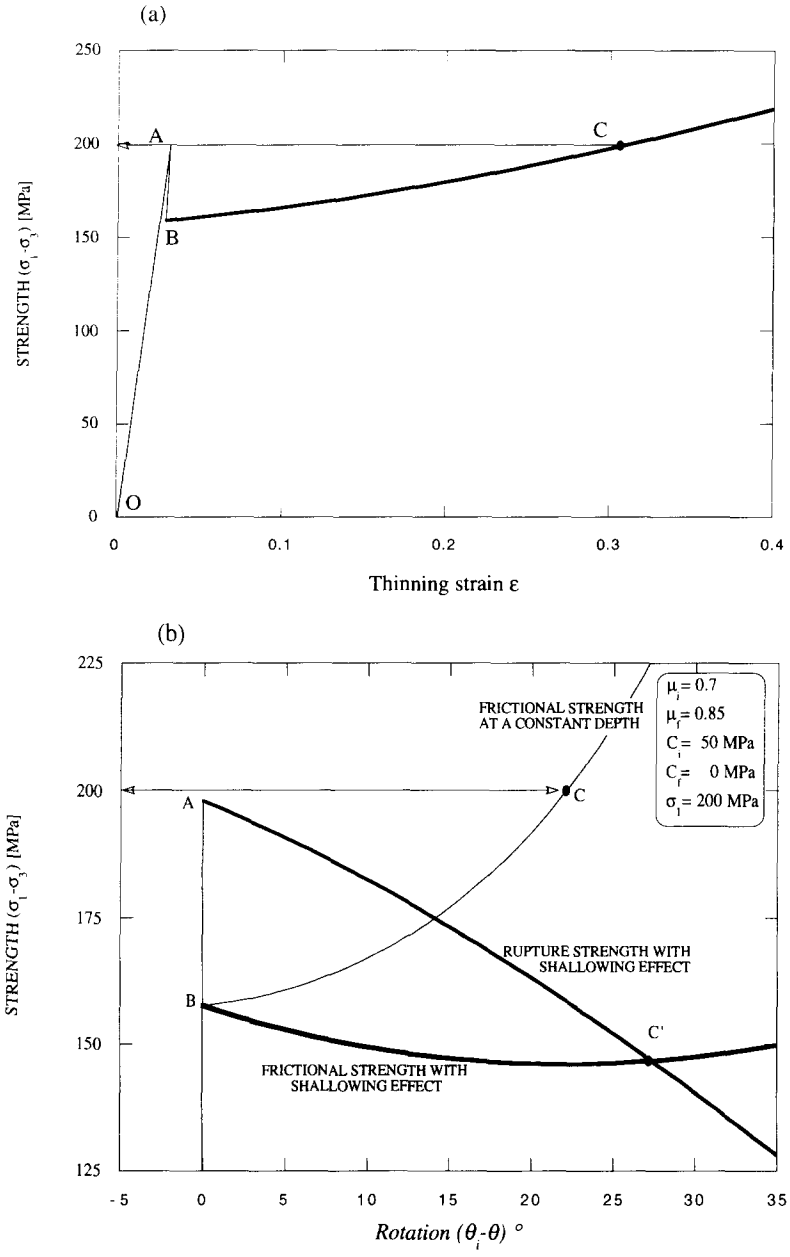

Fig. 6. The stress cycle under frictional rheology. (a) Stress-strain relation for an initially intact rock that deforms elastically (O–A), by rupture of a fault set (A–B), and by fault rotation, assuming constant fault length (B–C). (b) Softening due to shallowing (see text). Thin curve, calculated for a constant depth, reaches the level of rupture stress (horizontal arrows) at 23° tilt (Point C). Lower bold curve accounts for shallowing assuming a constant fault length. Thin curve shows the effect of shallowing on the intact rupture strength (Eqs. 4–5). The curves cross at the instability point, at 27° (point C'). The horizontal principal stress σ_3 becomes negative at 25°. (c) Mohr construction for the effect of shallowing.

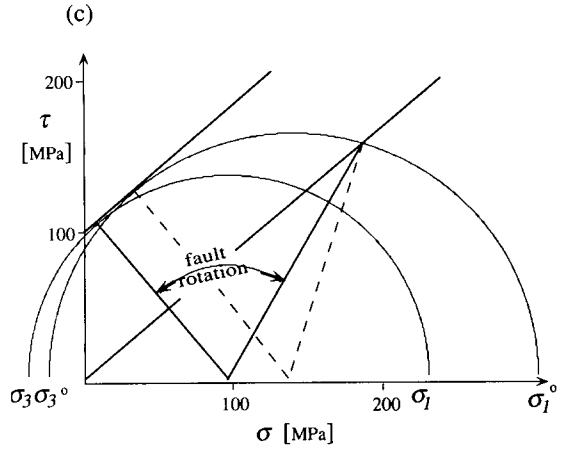

Fig. 6 (continued).

mean initial fault angle in the experiments $\theta_i = 27° \pm 5°$ does not differ significantly from the $\theta_{min} = 25°$ for (2a) and $\theta_{min} = 30°$ for (2b). Second, the mean stress ratio required to break an intact rock specimen $\sigma_1/\sigma_3 \approx 7 \pm 2$ is larger than the stress ratio required to slip an existing fault with the same orientation.

These two observations are not surprising. In terms of the Mohr yielding envelope, the first observation implies that the 'internal friction' of intact rocks is similar to the coefficient of friction of an existing fault, $\mu_i \approx \mu_f$. The second observation implies that the cohesion of an intact rock is larger than the cohesion of an existing fault ($C_i > C_f$) (Fig. 3). These observations form the basis for our estimate of frictional rheology of upper crustal rocks.

Consider a fault that forms within the ranges of σ_1/σ_3 and θ_i indicated by the cross in Fig. 4 (7 ± 2 and $27° \pm 5°$ respectively). The onset of faulting reduces the strength to the frictional strength to $\sigma_1/\sigma_3 \approx 4 \pm 1$ (between the curves of Fig. 4). Frictional sliding on this fault with the ensuing rotation cause strength increase along the appropriate frictional curve. The fault will lock once the rotation equates the frictional strength to the intact strength, following a rotation of 15°–30° from the initial fault (points B and C in Fig. 4). Further strain will require rupture of a new fault at θ_i.

Work-hardening

Fig. 5a shows calculated work-hardening due to fault rotations for a range of parameters, and Fig. 5b shows an example for a Mohr construction for rotations at a constant σ_1. The upper pair of curves are for a depth of about 11 km and the lower pair are for a depth of about 7.5 km (dry rock). Byerlee's law (Eq. 2a) is assumed for all calculations. The circle on each curve corresponds to the stress and the rotation at failure according to the respective intact strength (see legend). The high rotation for the lowest curve is not realistic. The normal stress for rupture in that curve is negative 20 MPa, a state of stress which is likely to exceed the tensional cracking strength.

Fig. 6a shows an example of a stress-strain relation for the frictional rheology. The relation is composed of an elastic pre-rupture region O–A, rupture of a fault set in the region A–B, and fault rotation in the region B–C. The fault rotation strength is calculated versus rotation (θ_i–θ) as in Fig. 5a, and the strain shown is thinning, assuming the length of a fault is conserved. The depth of a point on a fault that dips at dip θ is given by:

$$H(\theta) = H_o \frac{\sin \theta}{\sin \theta_i} \tag{4}$$

where H_o is the initial depth (Fig. 2). Therefore, the thinning strain ϵ is given by:

$$\epsilon(\theta) = \ln \frac{\sin \theta_i}{\sin \theta} \tag{5}$$

The sector B–C on the stress-strain curve of Fig. 6a corresponds to a 22° rigid-block rotation from $\theta_i = 65°$ at B to $\theta = 43°$ at C. Maintaining slip for $\theta < 43°$ requires larger stresses than that required at smaller rotations. Therefore, the post-rupture deformation of sector B–C in Fig. 5a is a work-hardening stage. The rotation and work-hardening will continue as far as the stresses required to maintain slip are smaller than the stresses required to rupture the intact rock (the stress that corresponds to point A in Fig. 6a). When work-hardening reach this level at point C, a new set of faults initiates at $\theta_i = 65°$ and the stress drops.

Nur et al. (1986) found that the angle of maximum active rotation varies between 20° and 45°

for a reasonable range of mechanical properties (C_f/C_i, μ and θ). Garfunkel (1989, fig. 6) explored the effects of varying μ and θ, as well as the pore pressure, on the maximal angles of rotation by strike slip. He adopts C_i of 100 MPa, and showed that pore pressure and the uncertainty in μ give a small effect, increasing the allowed rotation by a few degrees. The most significant uncertainty lies in the cohesion. Allowing a wide range of frictional properties he has evaluated the maximal rotation around the vertical axis to be between 15° and 40°. The present analysis gives a similar range of rotation angles for normal faults.

The effect of shallowing

Crustal extension and thinning decrease the depth and hence the lithostatic load σ_1. Fig. 6b shows strength–rotation relation accounting for a thinning strain calculated conserving the length of the fault in the plane of deformation. In the absence of sedimentation, the shallowing of (Eq. 4) and thinning (Eq. 5) are lower bounds on the actual values. Additional shallowing may result from intra-block thinning (cross-cutting secondary faults, ductile deformation, or erosion).

Fig. 6b shows the effect of shallowing on a single work-hardening stage. The thin curve shows the work-hardening without shallowing effect, under the rupture limit of 200 MPa (arrows), calculated from Eq. (2) with a constant σ_1 (same as in Fig. 6a). The lower bold curve in Fig. 6b is calculated from the same equation, but with $\sigma_1 = P_o \sin(\theta)/\sin(\theta_i)$, where P_o is the initial effective lithostatic stress (Eq. 4). This curve indicates initial softening (curve B–C′) that could apparently lead to rotations larger than 45°. However, as the strength of the intact rock decreases even faster (curve A–C′), second-generation faults will rupture after 27° rotation (C′) due to the softening of the intact rock. Fig. 6c illustrates the effect of shallowing by a Mohr construction.

2.5. Strength of a crustal plate: evolution from intact to multi domain

The repetition of the A–B–C described in Fig. 6a generates a 'saw-tooth' stress-rotation curve of Fig. 7. Each vertical segment (AB, CD, EF) corresponds to rupture of a new generation of faults. This saw-tooth response is valid under a constant σ_1, a requirement that does not hold, in general, for an extending crust (see above).

Fig. 8 illustrates two modes of faulting that might correspond to the stress-rotation curve of

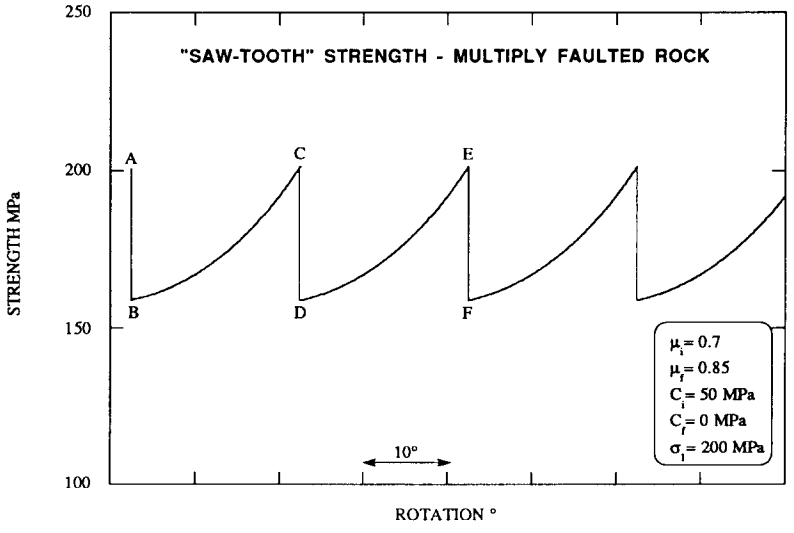

Fig. 7. Stress-rotation relation for a faulted plate under frictional rheology. Note the 'saw-tooth' shape response to high rotations, σ_1 is constant.

Fig. 7. In the first mode, the active zone locks and the new sets of faults rupture an adjacent zone in the crust (sequence *i–ii–iii*). In the second mode, newly formed second-generation fault sets cross-cut the locking rotated set (sequence *i–iv–vi*). The selection rules between the modes are related to additional hardening mechanisms, as well as strength and thickness irregularities, not accounted in the present idealized treatment. The integration of the two modes leaves a finite deformation such as illustrated in the bottom of Fig. 8 (*vi*).

For applying the model to a crustal plate, one needs to consider the ductile lower crust. At the present application we refer to the lower crust as having a constant strength that just shifts the strength-rotation curve (Fig. 7) by a constant. Such a shift does not modify the above behavior. Incorporation of the transient rheology of the lower crust is discussed elsewhere (Agnon and Reches, 1991; Reches and Agnon, 1992).

3. Discussion

3.1. Field observations

We discuss here some implications of the frictional rheology introduced above for common field observations in extended regions. These observations include rotations of active fault sets,

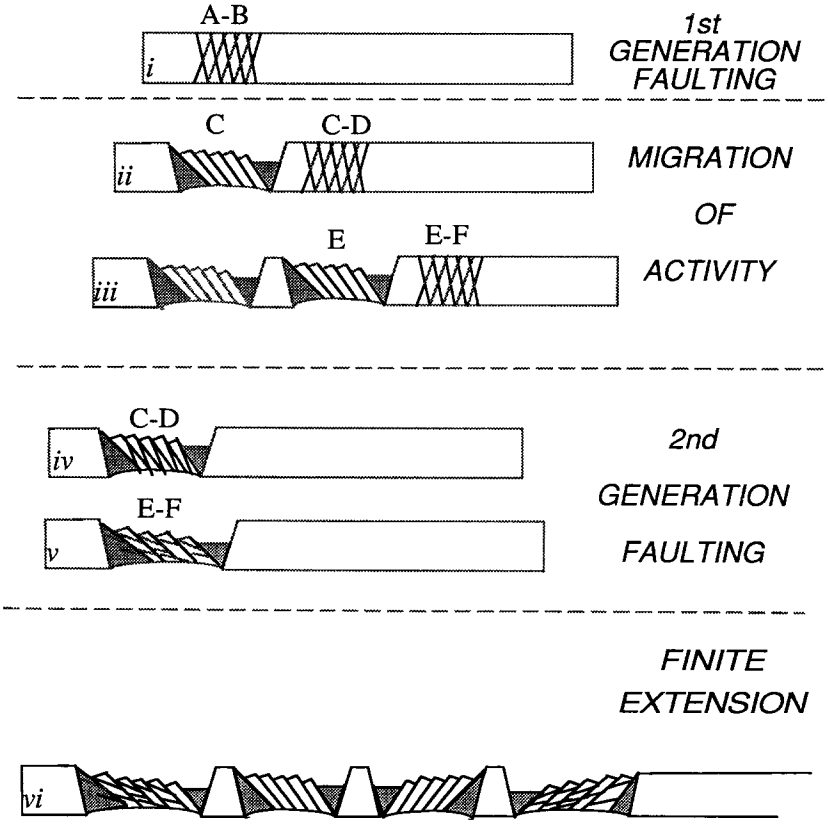

Fig. 8. Modes of extension by fault domain rotation: (*i*) onset of faulting in a domain, the width of which on the order of the thickness of the seismogenic crust; (*ii*) faults rotated to unfavorable dips and a new domain is forming adjacent to the locking domain; (*iii*) further migration of faulting and rotation; (*iv*) faults have rotated to unfavorable angles and second generation faults rupture the domain; (*v*) fault from second generation rotate to unfavorable dips; (*vi*) extended region with mixed mode rotations.

second-generation faulting, and migration of deformation.

Seismicity at intermediate to low-angle faults: Jackson (1987) has reviewed a global (continental) set of large ($M_s > 5.5$) normal faulting earthquakes. The distribution of dip of nodal planes from fault-plane solutions of these earthquakes (82 events) peak at 40°–50°, and the peak is stronger for fault planes in the subset for which this plane is detectable (15 events). Thatcher and Hill (1991) summarized additional data, and inferred that most of the large earthquakes cluster around 45° dipping planes. These studies propose that the originally steeper planes (dip ≈ 60°) have rotated and currently cause the pronounced activity on the intermediate–low-angle fault planes. Observed rotations of 15°–30° of the most active fault planes, from $\theta_i \approx 60°$ to $\theta \approx 45°–50°$ (Jackson, 1987; Thatcher and Hill, 1991; Anders et al., 1993) agree well with rotations predicted by our analysis using well accepted values of friction angle (Figs. 5–6).

Tilt Distributions and Multiple Sets: Fig. 9 shows the distribution of the tilt angles measured in bedding surfaces in the Basin and Range province by Stewart (1980). About 85% of the tilt angles of the blocks are distributed almost uniformly below 32° (group I in Fig. 9). One may also note a quasi-uniform distribution of tilts, at a significantly lower frequency, in the range 32°–52° (group II in Fig. 9), and very few blocks tilted above 57° (group III). Large block tilt beyond the fault locking angles, presumably occurs by successively created fault generations at optimal angle (Figs. 1, 5–8) (Proffett, 1977). The second-generation faults becomes active and rotates, while increasing the rotations of the primary set. Further rotation may be achieved on a third-generation set (Fig. 1). Ron et al. (1990) infer up to 41° rigid-block rotation on a single active set of strike-slip faults set along the Dead Sea Transform. Additional rotations have generated second-generation (and perhaps third-generation) fault sets.

As pointed out by previous authors, the uncertainties in material properties prohibit a well-defined prediction for the limiting rotation angles of active normal faults. Yet, the commonly accepted

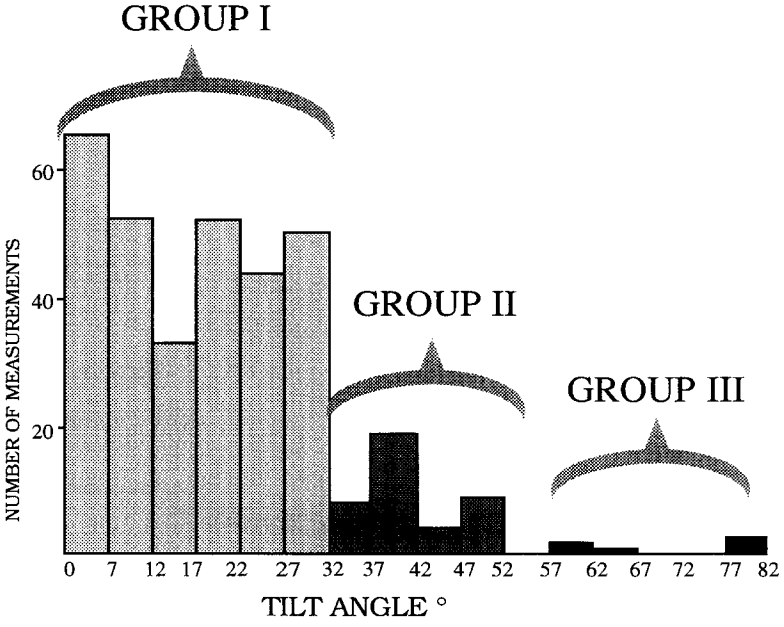

Fig. 9. Distribution of tilt angles of the Basin and Range blocks (after Stewart, 1980).

values for material properties give predictions in semi-quantitative agreement with observations. Consider Garfunkel's effective $C_i = 100$ MPa, and Sibson's (1985) average values, $C_f = 0$, $\mu_i = \mu_f = 0.75$. The maximum rotation for these values is 32° (with a constant maximum compression), in good agreement with the seismicity observations discussed above. Therefore, the uniform frequency of fault rotations between 0 and 32° (Fig. 9, group I) suggests variability in mechanical properties across domains.

We interpret the angle of block tilt as an indication to the range of rotation within which work-hardening was sufficient to drive the deformation away to an adjacent domain. The drop in frequency of tilts beyond 32° suggests that only a fraction of the domains in the Basin and Range province have undergone second-generation faulting (the style of Fig. 1a-b; Proffett, 1977). Further, the few domains tilted 57°–82° suggest that third-generation faulting occurred in even fewer domains (Fig. 1c).

The distribution in Fig. 9 suggests instabilities: domains that tilt beyond 32° and 52°, respectively, soften considerably and absorb much of the extension by large rotations. Such an instability can be related to the generation of secondary sets. A further instability by third-generation faulting may explain the low abundance of group III tilts (Fig. 9). These highly tilted domains localize extension, being the 'weakest link in the chain'. But the question remains regarding why a secondary set should be weaker than a new fault set on an adjacent block. To answer to this question one has to consider the contribution of the ductile deeper rocks in the plate to strength (Kusznir and Park, 1987; Sonder, 1989; Buck, 1991; Agnon and Reches, 1991; Reches and Agnon, 1992), that is beyond the scope of the present model.

The amount of rotation is bounded by Eq. (3) which is devised specifically for extensional faulting. Sibson (1985) points out that the stress ratio increase to infinity at rotations $\approx 30°$, if the mean stress in the plane of deformation is kept constant. This, however, is not a concern during normal faulting where the vertical normal stress is depth controlled. The stress ratio can physically approach infinity as the least compression tends to zero. The only practical limitations on reactivation of rotated normal faults are the shear strength of intact rock (Fig. 6c) and its tensional fracture strength (Le Pichon and Chamot-Rooke, 1991).

Migration of activity: Zoback et al. (1980) have delineated large-scale, long-term migration of extension in the Basin and Range. Wallace (1984, 1987) has demonstrated migration of faulting activity in the Basin and Range with spatial resolution of individual block and temporal resolution of decades. Other extensional terrains show migration of deformation as well (e.g., Angelier et al., 1982). In the present treatment it is work-hardening that drives migration of activity. If an active domain work hardens, it will lock once it becomes harder than another domain that is poised for yielding. The incumbent active domain releases the load and absorb the extension. Since it is the load instability that controls localization versus migration, the hardening calculated here is insufficient for locking. The effect of thinning on the cross-sectional area and frictional resistance overcomes hardening. Therefore, hardening mechanisms in the ductile part of the lithosphere are likely to work in regions of distributed deformation.

3.2. *The present frictional rheology model versus previous models*

The Mohr–Coulomb strength envelope is similar to conventional plastic yield surfaces in that only a part of the deforming body is undergoing deformation at any given instance. The rest of the body is elastic, and can be treated rigid in considering large strains (e.g., Cotrell, 1953). The important difference between continuum plasticity and the frictional rheology is due to the strength difference between intact and faulted rock. This strength difference drives fault-plane rotation. Slip-plane rotation is well known in crystal plasticity, but in that case it is lattice anisotropy that drives rotation (Cotrell, 1953; Lister et al., 1978; Takeshita et al., 1990; Ribe and Yu, 1991). The anisotropy generated by fault sets in the brittle crust is distinct from lattice anisotropy in that it is

generated by deformation (Reches, 1978), and therefore, it depends on the deformation path.

The term 'plate' is normally reserved for lithospheric blocks, but a few lines of evidence suggest that in highly extended regions the crust is decoupled from the mantle lithosphere. The lower crust is often inferred to form a weak channel between the upper crust and the mantle lithosphere (Kruse et al., 1991). Geological structures and stratigraphy of metamorphic core complexes suggest large displacements of an 'upper brittle plate' above a semi ductile layer (Crittenden et al., 1980). The low flexural rigidity inferred for extended regions further supports the notion of decoupling (Kusznir, 1991; Ebinger et al., 1991). Another indication for decoupling between the block tectonics of the shallow crust and the more continuous deformation in the substratum is the opposing sense of rotations (around horizontal as well as vertical axes) of adjacent domains frequently observed (Stewart, 1980; Ron et al., 1984). If decoupling is insufficient, upper crustal blocks are embedded passively in a large-scale flow of the lithosphere (England and Jackson, 1989; Molnar, 1992). In such cases our analysis is incomplete, since we have assumed the plate is loaded at its ends.

Agnon and Eidelman (1991) have alluded to hardening by crustal block rotation as a mechanism that might control necking instabilities. The present approach is different in that we focus on instability in the stress rather than in the load. The effect of shallowing on the frictional strength more than offsets the hardening at a given depth. Load-controlled necking instability in highly rotated domains will result, unless hardening from the ductile lower lithosphere can suppress the softening of the frictional upper crust (Agnon and Reches, 1991; Reches and Agnon, 1992).

Acknowledgement

We thank Z. Garfunkel for useful discussions and B. Vendeville for a thoughtful review of the manuscript. This research was supported by the Earth Science Administration of the Ministry of Energy and Infrastructure.

References

Agnon, A. and Eidelman, A., 1991. Lithospheric breakup in three dimensions: Necking of a work-hardening plastic plate. J. Geophys. Res., 96: 20189–20194.

Agnon, A. and Reches, Z., 1991. Strain hardening and continental extension: Rifting (Red-Sea mode) vs. denudation (Basin and Range mode). EOS, Am. Geophys. Union, Trans., 72, Fall Meet. Suppl., 450.

Anders, H.M., Spiegelman, M., Rodgers, D.W. and Hagstrum, J.T., 1993. The growth of fault-bounded tilt blocks. Tectonics, 12: 1451–1459.

Angelier, J., Lyberis, N., Le Pichon, X. and Huchon, P., 1982. The tectonic development of the Hellenic Arc and the Sea of Crete: A synthesis. Tectonophysics, 86: 159–196.

Brace, W.F. and Kohlstedt, D.L., 1980. Limits on lithospheric stress imposed by laboratory experiments. J. Geophys. Res., 85: 6248–6252.

Brun, J.P., Wenzel, F. and ECORS-DEKORP team, 1991. Crustal scale structure of the southern Rhinegraben from ECORS-DEKORP seismic reflection data. Geology, 19: 758–762.

Buck, W.R., 1991. Modes of continental lithospheric extension. J. Geophys. Res., 96: 20,161–20,178.

Byerlee, J.D., 1978. Friction of rocks. Pure Appl. Geophys., 116: 615–626.

Cotrell, A.H., 1953. Dislocations and Plastic Flow in Crystals. Clarendon Press, Oxford, England, 224 pp.

Crittenden, M.L., Coney, P.J. and Davis, G.H. (Editors), 1980. Cordilleran Metamorphic Core Complexes. Mem. Geol. Soc. Am., 153, 490 pp.

Dahlen, F.A., 1984. Noncohesive critical coulomb wedges; an exact solution. J. Geophys. Res., 89: 10,125–10,133.

Dietrich, J.H., 1981. Constitutive properties of faults with simulated gauge. Am. Geophys. Union, Geophys. Monogr., 24: 103–120.

Deverchere, J., Houdry, F., Solonenko, N.V., Solonenko, A.V. and Sankov, V.A., 1993. Seismicity, active faults and stress field of the North Muya region, Baikal Rift; new insights on the rheology of extended continental lithosphere. J. Geophys. Res., 98: 19,895–19,912.

Doser, I.D. and Yarwood, R.R., 1993. Deep crustal earthquakes associated with continental rifts. Tectonophysics, 229: 123–131.

Ebinger, C.J., Karner, G.D. and Weissel, J.K., 1991. Mechanical strength of extended continental lithosphere: Constraints from the western rift system, East Africa. Tectonics, 10: 1239–1256.

England, P. and Jackson, J., 1989. Active deformation of the continents. Annu. Rev. Earth Planet. Sci., 17: 197–226.

Eyal, M., Eyal, Y., Bartov, Y. and Steinitz, G., 1981. The tectonic development of the western margin of the Gulf of Elat (Aqaba) Rift. Tectonophysics, 80: 39–66.

Fletcher, R.C. and Hallet, B., 1983. Unstable extension of the lithosphere: A mechanical model for Basin and Range structure. J. Geophys. Res., 88: 7457–7466.

Freund, R., 1974. Kinematics of transform and transcurrent faults. Tectonophysics, 21: 93–134.

Garfunkel, Z., 1974. Model for late Cenozoic tectonic history of the Mojave Desert, California, and for its relations to adjacent regions. Geol. Soc. Am. Bull., 85: 1931–1944.

Garfunkel, Z., 1989. Regional deformation by block rotation and translation. In: C. Kissel and C. Laj (Editors), Paleomagnetic Rotations and Continental Deformation. NATO Advanced Workshop, Kluwer, pp. 181–208..

Garfunkel, Z. and Bartov, Y., 1977. The tectonics of the Suez Rift. Geol. Surv. Israel Bull., 71: 44 pp.

Goetze, C. and Evans, B.E., 1979. Stress and temperature of the bending lithosphere as constrained by experimental rock mechanics. Geophys. J. R. Astron. Soc. London, 59: 463–478.

Handin, J., 1966. Strength and ductility. In: S.P. Clark (Editor), Handbook of Physical Constants. Mem. Geol. Soc. Am., 97: 223–289.

Handin, J., 1969. On the Coulomb–Mohr failure criterion. J. Geophys. Res., 74: 5343–5348.

Jackson, J.A., 1987. Active normal faulting and crustal extension. In: M.P. Coward, J.F. Dewey and P.L. Hancock (Editors), Continental Extensional Tectonics. Geol. Soc. London, Spec. Publ., 28: 3–17.

Jackson, J.A., White, N.J., Garfunkel, Z. and Anderson, H., 1988. Relations between normal -fault geometry, tilting and vertical motions in extensional terrains: an example from the southern Gulf of Suez. J. Struct. Geol., 10: 155–170.

Jaeger, J.C. and Cook, N.G.W., 1979. Fundamentals of Rock Mechanics, 3rd edition. Chapman and Hall, London.

Kruse, S., McNutt, M., Phipps-Morgan, J., Royden, L. and Wernicke, B., 1991. Lithosphere extension near Lake Mead, Nevada: A model for ductile flow in the lower crust. J. Geophys. Res., 96: 4435–4456.

Kusznir, N.J., 1991. Lithosphere flexural strength and effective elastic thickness during continental extension. Terra Abstr., 3: 261–262.

Kusznir, N.J. and Park, R.G., 1987. The extensional strength of the continental lithosphere: its dependence on geothermal gradient, and crustal composition and thickness. In: M.P. Coward, J.F. Dewey and P.L. Hancock (Editors), Continental Extensional Tectonics. Geol. Soc. London, Spec. Publ., 28: 35–52.

Le Pichon, X. and Chamot-Rooke, N., 1991. Extension of continental crust. In: D.W. Mueller, J.A. McKenzie and H. Weissert (Editors), Controversies in Modern Geology; Evolution of Geological Theories in Sedimentology, Earth History and Tectonics. Eidg. Tech. Hochschule, Zurich, pp. 313–338.

Lister, G.S., Patterson, M.S. and Hobbs, B.E., 1978. The simulation of fabric development in plastic deformation and its application to quartzite: The model. Tectonophysics, 45: 107–158.

McGarr, A., 1980. Some constraints on level of shear stress in the crust from observations and theory. J. Geophys. Res., 85: 6231–6138.

Molnar, P., 1992. Brace–Goetze strength profiles, the partitioning of strike-slip and thrust faulting at zones of oblique convergence, and the stress-heat flow paradox of the San Andreas fault. In: B. Evans and T. Wong (Editors), Fault Mechanics and Transport Properties of Rocks. Academic Press, London, pp. 435–459.

Nur, A., Ron, H. and Scotti, O., 1986. Fault mechanics and the kinematics of block rotations. Geology, 14: 746–749.

Oertel, G., 1965. The mechanisms of faulting in clay experiments. Tectonophysics, 2: 243–393.

Proffett Jr., J.M., 1977. Cenozoic geology of the Yerington district, Nevada, and implications on the nature and origin of Basin and Range faulting. Geol. Soc. Am. Bull., 88: 247–266.

Reches, Z., 1978. Analysis of faulting in three-dimensional strain field. Tectonophysics, 47: 109–129.

Reches, Z., 1979. Deformation of foliated media. Tectonophysics, 57: 119–129.

Reches, Z., 1988. Evolution of fault patterns in clay experiments. Tectonophysics, 145: 141–156.

Reches, Z., 1994. How rigid are rigid blocks?, EOS, Trans. Am. Geophys. Union, Fall Meet. Suppl., 74 (43): 207.

Reches Z. and Agnon, A., 1992. Transient rheology (hardening/softening) of the lithosphere and its effect on lithosphere extension. EOS, Trans. Am. Geophys. Union, Fall Meet. Suppl., 73: 307.

Reches, Z. and Lockner, D., 1994. Nucleation and growth of faults in brittle rocks. J. Geophys. Res., 99: 18,159–18,173.

Ribe, N.M. and Yu, Y., 1991. A theory for plastic deformation and textural evolution of olivine polycrystals. J. Geophys. Res., 96: 8325–8335.

Roberts, A.M. and Yielding, G., 1991. Deformation around basin-margin faults in the North Sea/mid-Norway rift. In: A.M. Roberts, G. Yielding and B. Freeman (Editors), The Geometry of Normal Faults. Geol. Soc. London, Spec. Publ., 65: 61–78.

Ron, H., Freund, R., Garfunkel, Z. and Nur, A., 1984. Block rotation by strike-slip faulting: Structural and paleomagnetic evidence. J. Geophys. Res., 89: 6256–6270.

Ron, H., Nur, A. and Eyal, Y., 1990. Multiple strike-slip fault sets: A case study from the Dead Sea Transform. Tectonics, 9: 1421–1431.

Scholz, C.H., 1990. The Mechanics of Earthquakes and Faulting. Cambridge University Press, New York, 439 pp.

Sibson, R.H., 1985. A note on fault reactivation. J. Struct. Geol., 7: 751–754.

Smith, R.B., Nagy, W.C., Julander, K.A., Viverios, J.J., Barker, C.A. and Gants, D.G., 1989. Geophysical and tectonic framework of the eastern Basin and Range–Colorado Plateau– Rocky Mountain transition. In: L.C. Pakiser and W.D. Mooney (Editors), Geophysical Framework of the Continental United States. Geol. Soc. Am. Mem., 172: 205–233.

Sonder, L.J. and England, P., 1986. Vertical averages of rheology of the continental lithosphere: relation to thin sheet parameters. Earth Planet. Sci. Lett., 77: 81–90.

Stein, R.S. and Barrientos, S.E., 1985. Planar high-angle faulting in the Basin and Range; geodetic analysis of the 1983 Borah Peak, Idaho, earthquake. J. Geophys. Res., 90:11,355–11,366.

Stesky, R.M., Brace, W.F., Riley, D.K. and Robin, P.Y.F.,

1974. Friction in faulted rock at high temperature and pressure. Tectonophysics, 23: 177–203.

Stewart, J.H., 1980. Regional tilt patterns of late Cenozoic basin-range fault blocks, western United States. Geol. Soc. Am. Bull., 91: 460–464.

Takeshita, T., Wenk, H.R., Canova, G.R. and Molinari, A., 1990. Simulation of dislocation-assisted plastic deformation in olivine polycrystals. In: D.J. Barber and P.G. Meredith (Editors), Deformation Processes in Minerals, Ceramics and Rocks. Univ. Essex, UK, pp. 365–374.

Thatcher, W. and Hill, D.P., 1991. Fault orientation in extensional and conjugate strike-slip environments and their implications. Geology, 19: 1116–1120.

Thompson, G., Catchings, R., Goodwin, E., Holbrook, S., Jarchow, C., Mann, C., McCarthy, J. and Okaya, D., 1989. Geophysics of the western Basin and Range province. In: L.C. Pakiser and W.D. Mooney (Editors), Geophysical Framework of the Continental United States. Geol. Soc. Am. Mem., 172: 177–203.

Wallace, R.E., 1984. Patterns and timing in late Quaternary faulting in the Great Basin province and relations to some regional tectonic features. J. Geophys. Res., 89: 5763–5769.

Wallace, R.E., 1987. Grouping and migration of surface faulting and variations in slip rates on faults in the Great Basin province. Bull. Seismol. Soc. Am., 77: 868–876.

Westaway, R., 1991. Continental extension on sets of parallel faults: observational evidence and theoretical models. In: A.M. Roberts, G. Yielding and B. Freeman (Editors), The Geometry of Normal Faults. Geol. Soc. London, Spec. Publ., 65: 143–169.

Yielding, G., Badley, M.E. and Freeman, B., 1991. Seismic reflections from normal faults in the northern North Sea. In: A.M. Roberts, G. Yielding and B. Freeman (Editors), The Geometry of Normal Faults. Geol. Soc. London, Spec. Publ., 65: 79–89.

Zoback, M.L., Anderson, E. and Thompson, G., 1980. Cainozoic evolution of the state of stress and style of tectonism of the Basin and Range province of the western United States. Philos. Trans. R. Soc. London, Ser. A, 300: 407–434.

Zuber, M.T., Parmentier, E.M. and Fletcher, R.C., 1986. Extension of continental lithosphere; a model for two scales of Basin and Range deformation. J. Geophys. Res., 91: 4826–4838.